Check for updates

A novel water-soluble naked-eye probe with a large Stokes shift for selective optical sensing of Hg²⁺ and its application in water samples and living cells†

Yingying Zhang,‡[a] Chao Zhang,‡[a] Yingnan Wu,‡[b] Bing Zhao,‡[a] Liyan Wang‡[a] and Bo Song [ID] ‡*[a]

A water-soluble and colorimetric fluorescent probe with a large Stokes shift (139 nm) for rapidly detecting Hg²⁺, namely **Hcy-mP**, was synthesized by using an indole derivative and 2,4-dihydroxybenzaldehyde as starting materials. This probe demonstrates good selectivity for Hg²⁺ over other metal ions including Ag⁺, Pb²⁺, Cd²⁺, Cr³⁺, Zn²⁺, Fe³⁺, Co²⁺, Ni²⁺, Cu²⁺, K⁺, Na⁺, Mg²⁺, and Ca²⁺ in aqueous solution. With the increase in concentration of Hg²⁺, the color of the solution changed from pale yellow to pink and the fluorescence intensity decreased slightly. When 5-equivalents of EDTA were added to the solution with Hg²⁺, the fluorescence intensity of this probe was restored. The probe has been applied to the detection of Hg²⁺ in real water samples. Moreover, this probe was confirmed to have low cytotoxicity and excellent cell membrane permeability. The effect of **Hcy-mP**–Hg²⁺ towards living cells by confocal fluorescence was also investigated.

Introduction

Among heavy metal cations, Hg²⁺ is one of the most toxic and dangerous ions even at a low concentration. Hg²⁺ pollution was caused by many natural and human factors to a large extent, and is harmful to living creatures.[1,2] Once the organism is exposed to a Hg²⁺ environment, a variety of severe health problems arise.[3,4] For instance, Hg²⁺ can disturb some metabolic processes involving proteins and enzymes.[5] And Hg²⁺ has been recognized as one of the reason for various cognitive and motion disorders, as well as prenatal brain damage and DNA lesions.[6-9] Hg²⁺ can be accumulated through the food chain and subsequently affect people's health.[10] Thus, it is important for us to develop a useful, efficient and sensitive approach to detect Hg²⁺.

Currently, there are many available ways to detect Hg²⁺, but the fluorescence-based approach has attracted more attention.[11-15] In recent years, fluorescent probes were used as cation sensors due to their significant advantages such as high sensitivity and selectivity, and rapid response for analytical, biomedical and environmental science.[16-18] They were also found to be applied in analytical, biomedical and environmental science.[19] However, most of the inventive probes have some drawbacks. For example, the synthesis

process of some probes is relatively complex, and the post-processing is cumbersome.[20-23] Lots of probes not only have poor aqueous solubility but also have short emission wavelength, which are both shortcomings that can cause a certain degree of damage towards cells.[24,25] Considering these shortcomings of the currently applied probes and the extreme toxicity of Hg²⁺, it is imperative to develop more fluorescent sensors with long emission wavelengths, low toxicity and simple synthesis methods for the rapid detection of Hg²⁺ in the environment and biological systems.

On this basis, a simple fluorescent probe based on an indole ring, 2-(2,4-dihydroxystyrene)-3,3-dimethyl-3*H*-indole-5 potassium sulfonate (**Hcy-mP**) was designed and synthesized. This probe can be used to detect Hg²⁺ in aqueous solutions by fluorescent analyses with high selectivity and sensitivity, distinguishing it from other common cations. In the Hg²⁺ recognition process, the color of the probe solution changed obviously from light yellow to pink, which can be recognized clearly by the naked eye. Moreover, the selective detection of probe **Hcy-mP** towards Hg²⁺ was completely reversible upon the addition of EDTA. Then, the probe was successfully used for detection of Hg²⁺ in water samples. **Hcy-mP** performed well in the biological experiments, demonstrating that this probe can be applied to detect intracellular Hg²⁺ (Scheme 1).

Results and discussion

Synthesis

A sulfonate group was introduced into the indole ring to improve the water solubility and the photostability of this

[a]*College of Chemistry and Chemical Engineering, Qiqihar University, Qiqihar 161006, Heilongjiang, China. E-mail: songboliu@sina.com; Tel: +86 13946272680*

[b]*Institute of Molecular Sciences and Engineering, Shandong University, Qingdao 266237, Shandong, China*

† Electronic supplementary information (ESI) available. See DOI: 10.1039/c9ra03924d

‡ These authors contributed equally to this work.
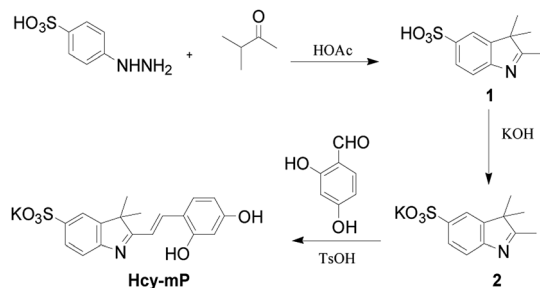
Scheme 1 The synthetic routes of probe **Hcy-mP**.

probe.[26] Compound 1 was synthesized by two steps and compound 2 was obtained by alkylating of compound 1 with KOH. Finally, the target compound **Hcy-mP** was obtained by reaction with aldehyde in 85% yield under acidic condition. The ^{1}H NMR of the final compound shows the peaks position of the hydroxyl group of the compound were around 11.07 ppm and 10.78 ppm, and the peaks position of the double bond were around 7.10–7.12 ppm (ESI†). These signs indicate that the target product has been successfully synthesized.

UV absorbance and fluorescence emission spectra of Hcy-mP

Owing to the sulfonate groups unit in **Hcy-mP**, this probe possesses a full-water solubility, so we investigated the spectra of probe **Hcy-mP** in 100% aqueous solution (pH = 7.0–7.4).

Under medium environment, fluorescence emission spectra of **Hcy-mP** exhibits the maximum at 517 nm with excitation at 378 nm, and large Stokes shift of 139 nm was observed (Fig. 1). The large Stokes shift of this probe with can reduce the self-absorption to avoid self-quenching and quantitative detection error from excitation light.

Cation-sensing properties

It is widely agreed that high selectivity is required for the probe to recognize the target ion from other various ions. The sensitivity of **Hcy-mP** was tested by mixed with different metal ions (20 μM) (Ag^+, Pb^{2+}, Cd^{2+}, Cr^{3+}, Zn^{2+}, Fe^{3+}, Co^{2+}, Ni^{2+}, Cu^{2+}, K^+, Na^+, Mg^{2+}, and Ca^{2+}), respectively. **Hcy-mP** exhibited excellent selectivity in both absorbance and emission spectra. With

addition of Hg^{2+}, the maximum UV-absorption of the probe was red-shift from 378 nm to 517 nm, as well as the absorbance declined (Fig. 2a) and the fluorescence intensity was significantly quenched at 517 nm with the fluorescence quantum yield (Φ) of 0.11 relative to rhodamine B solution (in methanol) (Fig. 2b). In contrast, the addition of other metal ions has little influence on the absorbance and fluorescence intensity of the probe. These results indicate that the probe could be used as an effective tool for detecting Hg^{2+}.

At the same time, the selectivity and anti-interference performance of this probe with other related metal cations were also investigated in the presence/absence of Hg^{2+}. As can be seen from Fig. 3, this probe shows significant higher selectivity for Hg^{2+} than other metal cations, which indicates that the specific response of **Hcy-mP** to Hg^{2+} was not disturbed by other cations.

Titration experiment

The fluorescence titration experiment was carried out by adding different concentrations of Hg^{2+} from 0–25 μM to **Hcy-mP** (10 μM) solution in HEPES buffer solution. As shown in Fig. 4a, the fluorescence intensity at 517 nm of **Hcy-mP** decreased gradually with the addition of Hg^{2+}. This result indicates that **Hcy-mP** has high selectivity to Hg^{2+}.

Fig. 2 (a) UV-vis spectra of **Hcy-mP** (10 μM) upon the addition of different metal ions (10 μM) in 100% HEPES buffer solution (pH = 7.0); (b) fluorescence spectra of **Hcy-mP** (10 μM) upon the addition of different metal ions (10 μM) in HEPES buffer solution (λ_{ex} = 378 nm, silt = 10 nm).
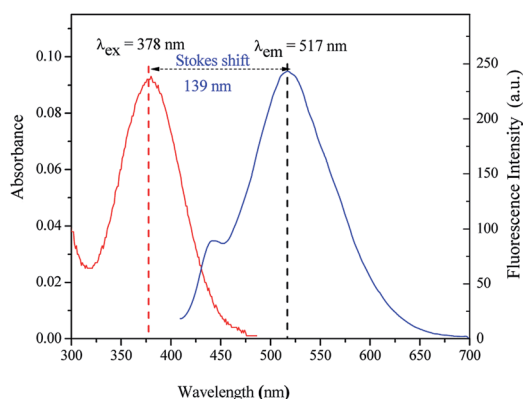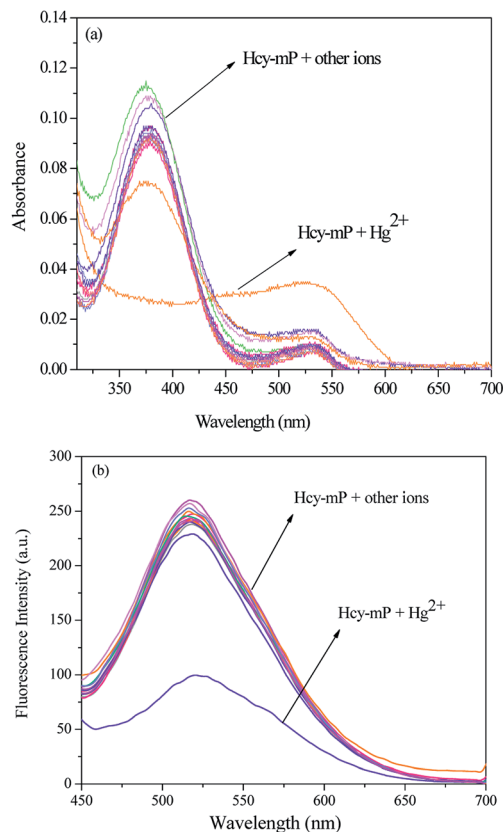

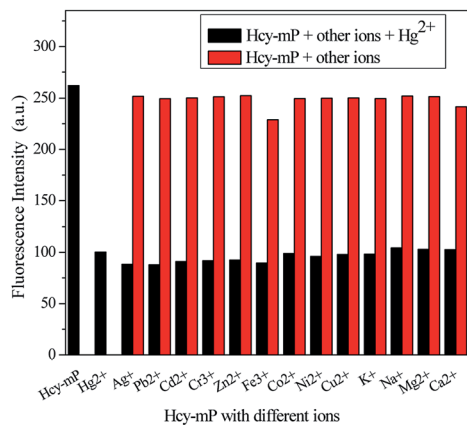**Fig. 1** Absorption and emission spectra of **Hcy-mP** (λ_{ex} = 378 nm, λ_{em} = 517 nm, Stokes shift = 139 nm).

Fig. 3 Fluorescence intensity of **Hcy-mP** (10 μM) upon addition of metal ions (20 μM) and addition of Hg^{2+} (10 μM) in HEPES buffer solution (λ_{ex} = 378 nm, silt = 10 nm).

In addition, the addition of Hg^{2+} changed the color of the solution from pale yellow to pink, indicating that this probe could be used for naked eye recognition. These phenomena prove that the qualitative and quantitative detection of Hg^{2+} can be achieved, respectively by this probe (Fig. 4b–d).

According to the Benesi–Hildebrand curve, the association constant (K_a) between the probe and Hg^{2+} was calculated to be 1.2×10^{-4} M^{-1} (R^2 = 0.9866) (Fig. S1†), which indicates that this probe has excellent binding ability to Hg^{2+}. By using the fluorescence titration experiment of **Hcy-mP** to Hg^{2+}, the detection limit was improved to as low as 1.08 μM (R^2 = 0.9914) (Fig. S2†). The detection limit is excellent value to detect the submillimolar concentration of the Hg^{2+} in many biological systems.

Sensitivity study

Reaction time and stability are important factors to assess the performance of a novel probe. The fluorescence intensity of **Hcy-mP** to Hg^{2+} was monitored in 2 h at λ_{ex} = 378 nm. As shown in Fig. 5, the fluorescence intensity of **Hcy-mP** with Hg^{2+} is

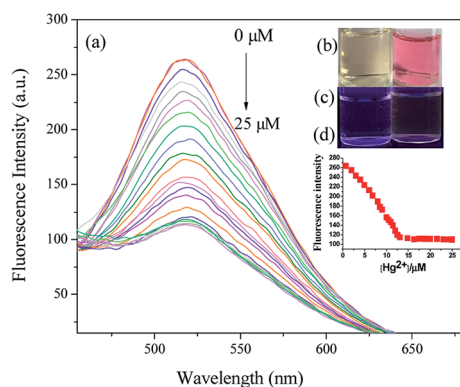**Fig. 4** (a) Effects of different concentrations of Hg^{2+} on the fluorescence spectra of **Hcy-mP** (10 μM) at different Hg^{2+} concentrations (from top to bottom Hg^{2+} concentrations are 0–25 μmol L^{-1}). (b) and (c) Naked-eye color of **Hcy-mP** solution in HEPES buffer in the absence (left, bright) or presence (right, fluorescence) of Hg^{2+} (20 μM). (d) The scatter diagram of the fluorescence titration experiment.
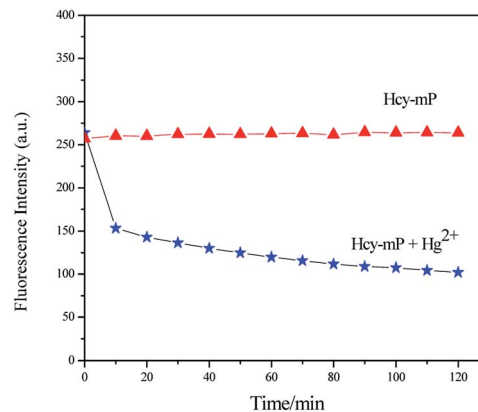

Fig. 5 Effect of reaction time on fluorescence emission spectra of **Hcy-mP** and **Hcy-mP** with Hg^{2+} (20 μmol L^{-1}).

quenched obviously in 10 min, slowed down in the following experimental time and kept steady, which indicate that this probe could rapidly identify Hg^{2+} in aqueous solution and can be used as a sensitive probe for environmental analysis.

EDTA experiment

The EDTA experiment was used to assess the reversibility of **Hcy-mP** with Hg^{2+} in HEPES (pH = 7.0) solution. When EDTA (10 μM) was added to solution of **Hcy-mP**–Hg^{2+}, the absorbance and fluorescence intensity were enhanced again in several seconds (Fig. 6a and b). Then added Hg^{2+} and then added EDTA again in following circles, similar changes were appeared in both absorbance and fluorescence intensity of the probe. These experiments illustrate that the coordination process is reversible. And fluorescence intensity changes of the probe at 517 nm when adding compounds (Hg^{2+} and EDTA) for 4 cycles prove that **Hcy-mP** can be used as a reversible fluorescence probe in practical application (Fig. 6c).

Effect of pH

Moreover, the fluorescent property of **Hcy-mP** in the absence and presence of Hg^{2+} were investigated at different pH values range from 2.0 to 12.0. As shown in Fig. S3,† when the pH value is between 2.0 and 5.0, the fluorescence intensity of **Hcy-mP** is similar to **Hcy-mP** with Hg^{2+}. At the pH values range from 5.0 to 11.0, the fluorescence intensity of **Hcy-mP** solution with Hg^{2+} was significantly lower than that of **Hcy-mP**. This result indicates that **Hcy-mP** could act as a fluorescence probe for detecting Hg^{2+} at a wide pH range.

Investigation of the binding mode

In order to speculate the Hg^{2+} recognition site on **Hcy-mP**, another compound **Hcy-pP** (Scheme 2) was synthesized. The synthesis routes of **Hcy-pP** were similar to **Hcy-mP** (ESI†). The fluorescence emission spectra of **Hcy-pP** (10 μM) with different metal cations (20 μM) were measured. As shown in Fig. 7, compared with the fluorescence intensity of **Hcy-pP**, fluorescence intensity of **Hcy-pP** solution with different metal cations was not increased obviously. This result shows that the presence of those ions have no influence on the fluorescence intensity of
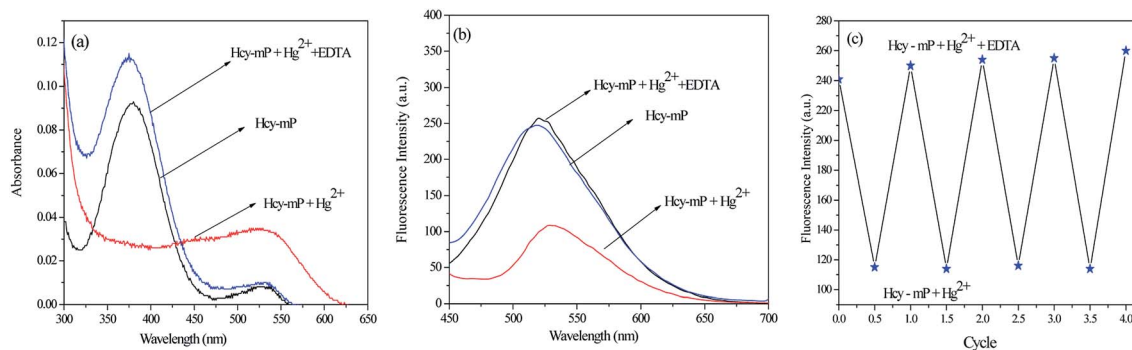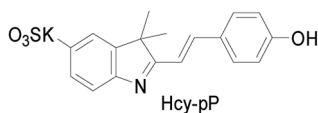
Fig. 6 (a) Absorption and (b) emission spectral changes of **Hcy-mP** (10 μM), after addition of Hg^{2+} (10 μM) and followed by EDTA (10 μM); (c) fluorescence intensity changes of **Hcy-mP** (10 μM) at 517 nm under addition of compounds (Hg^{2+} and EDTA) for 4 cycles (λ_{ex} = 378 nm).

probe **Hcy-pP**, which further indicates that the 4-hydroxy in the compound does not have impacts on **Hcy-mP** recognize the metal cations.

Then we studied the ESI-MS data of **Hcy-mP**–Hg^{2+}. As shown in Fig. S4 and S5,† from the ESI-MS (negative mode), the detection value of [**Hcy-mP** + Hg^{2+}]$^-$ is 559.0153 (m/z) (calc. = 558.9870), [**Hcy-mP** + Hg^{2+} + K$^+$ + H$^+$]$^+$ is 599.0763 (m/z) (calc. = 599.2904) which confirms the binding ration of the **Hcy-mP** with Hg^{2+} is 1 : 1.

In order to further study the binding mode of **Hcy-mP**–Hg^{2+}, job plot experiment also was conducted. As shown in Fig. 8, the fluorescence intensity at 517 nm was plotted against the [**Hcy-mP**]/[**Hcy-mP** + Hg^{2+}] (10 μM). The two lines intersected when the mole fraction of metal was 0.5 which indicates the binding ratio for the complex between **Hcy-mP** and Hg^{2+} is 1 : 1.

According to the current studies,[27–29] the mode of metal ions combine with the probe can be done based on ^{1}H NMR titration experiments, the binding mode of **Hcy-mP** with Hg^{2+} was

investigated by using this method. As shown in Fig. 9, the comparison of the ^{1}H NMR spectra of **Hcy-mP** and **Hcy-mP** mixed with 2 and 5 equivalent of Hg^{2+} tells that the 2′OH proton was gradually disappeared when Hg^{2+} (10 μM) was added to **Hcy-mP** solution which reveals that Hg^{2+} combines with the 2′OH oxygen of the probe.

Above research shows a 1 : 1 binding ratio for **Hcy-mP** mixture, the proposed structure of **Hcy-mP** complex was shown in Scheme 3.

Application in water samples

Due to the high sensitivity and excellent selectivity fluorescence properties of **Hcy-mP** for detecting Hg^{2+}, the probe **Hcy-mP** was further investigated for determination of Hg^{2+} in environment samples. These samples were spiked with Hg^{2+} at different concentrations, and the fluorescence responses of **Hcy-mP** toward all samples were examined by the fluorescence emission spectra, respectively. Each sample was analyzed with their three replicates. As shown in Table S1,† the results obtained of real samples shows good agreement with Hg^{2+} spiked samples. The probe shows excellent recovery in the range of 95–103% with the low relative standard deviations RSD (0.7–2.3%), indicating that the probe has high sensitivity and good reliability for determination of Hg^{2+} in practical samples of environment.

Scheme 2 The structure of **Hcy-pP**.

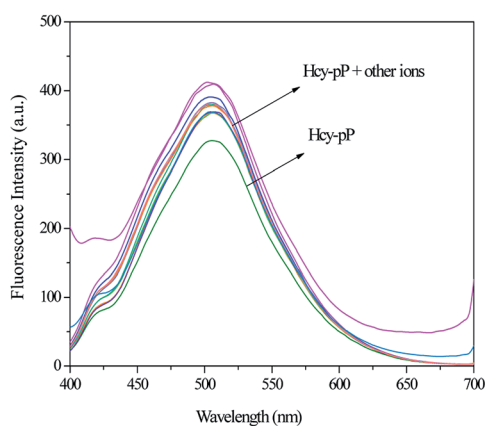**Fig. 7** Fluorescence spectra of **Hcy-pP** (10 μM) upon the addition of different metal ions (20 μM) in HEPES buffer solution.

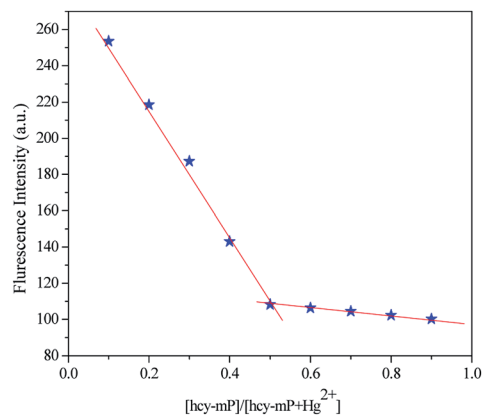**Fig. 8** Job plot of the **Hcy-mP**–Hg^{2+} mixture in HEPES (pH = 7.0) solution, keeping the total concentration of **Hcy-mP** and Hg^{2+} at 10 μM. The observed wavelength was 517 nm.

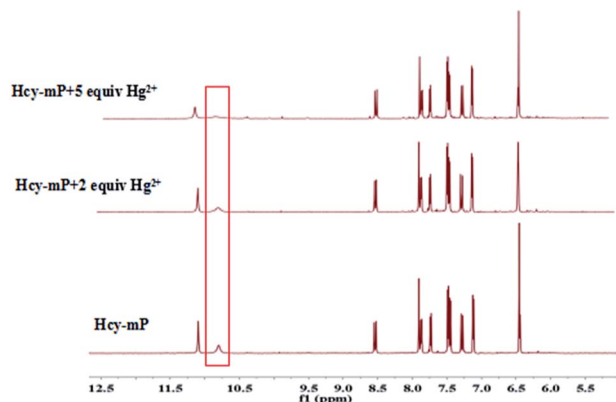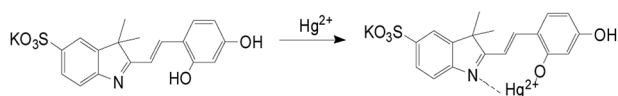**Fig. 9** The ^{1}H NMR for **Hcy-mP** and **Hcy-mP** + Hg^{2+} (2, 5 equiv.) in DMSO.

Scheme 3 Proposed sensing mechanism of **Hcy-mP** towards Hg^{2+}.

Cytocompatibility assay analysis

In order to investigate whether this probe can be applied in living cells, the cell compatibility of probe was first studied. Results are shown in Fig. 10.

The above result shows that the survival rates of HeLa cells decrease slightly with the increasing of probe concentrations (10 μM, 20 μM, 30 μM, 40 μM, 50 μM, 60 μM, 70 μM, 80 μM, 90 μM and 100 μM). The survival rate of HeLa cells is still greater than 85% when using high probe concentration, which indicates that the probe has high biocompatibility and low cytotoxicity. Therefore, the probe **Hcy-mP** can be employed in cell imaging for further investigation.

Intracellular confocal fluorescent imaging

Cell images were obtained using confocal fluorescence microscopy. Fluorescence images of HeLa cells labeled with **Hcy-mP** were monitored upon the excitation at 517 nm, as shown in Fig. 11b,
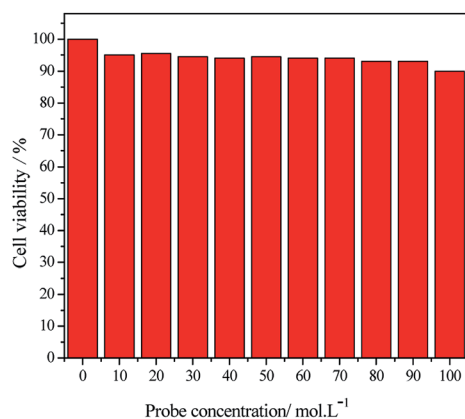

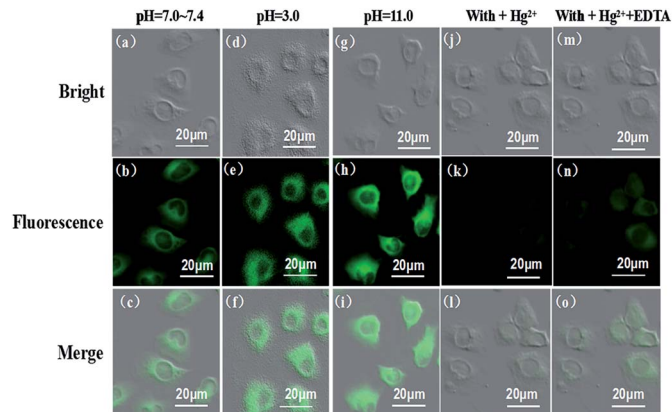**Fig. 10** Cell viability HeLa cells.

Fig. 11 Confocal microscopy images of 10 μM **Hcy-mP** in HeLa cells at pH 7.4, 3.0 and 11.0 (b, e and h) for 30 min Fluorescence images of cells were then further incubated with Hg^{2+} (10 μM) for 30 min (k). Cells were further treated with EDTA (10 μM) for 30 min. Bright field (a, d, g, j and m), fluorescence (b, e, h, k and n) and merged field (c, f, i, l and o). $\lambda_{ex} = 378$ nm.

e, h, k and n. HeLa cells were incubated with **Hcy-mP** (10 μM) in different pH values (pH 7.4, 3.0, 11.0) for 30 min at 37 °C. Bright field images were shown in Fig. 11a, d, g, j and m. It is worth noting that the merge of fluorescence and bright field images (Fig. 11c, f, i, l and o) confirmed that the fluorescence signal was only located in the intracellular area. Obviously, without the presence of Hg^{2+}, the fluorescence intensity of cells under acidic conditions (Fig. 11e) was stronger than neutral conditions (Fig. 11h), and the fluorescence intensity under alkaline condition was stronger than acidic condition, which indicates that the probe can be used in a wide pH value range. Then the treated cells were washed with PBS three times and incubated with $HgCl_2$ (20 μM) in culture medium (pH 7.4) (Fig. 11j). Bright green fluorescence appeared an apparently quenched in HeLa cells (Fig. 11k). As shown in Fig. 11n, the green fluorescence was restored in cells upon further treatment with EDTA (20 μM). Hence, the probe is cell membrane permeable and can be applied for detecting pH and Hg^{2+} in living cells.

Experimental sections

Material and apparatus

All chemical reagents and solvents were purchased from commercial suppliers and were used without further purification unless otherwise noted.

2,4-Dihydroxybenzaldehyde was purchased from Aladdin Reagent Co., Ltd. ^{1}H and ^{13}C NMR spectra were recorded on AVANCE 600 MHz NMR spectrometer (Bruker biospin, Switzerland). High resolution mass spectrometry (HRMS) data were obtained with Waters LCT Premier XE spectrometer (Waters, American). Absorption spectra were measured on TU-1901 double-beam UV-vis spectrophotometer (Beijing Purkinje General Instrument Co., LTD, Beijing, China). Fluorescence emission was detected on Varian Cary Eclipse (PerkinElmer, American) spectrophotometer. Fluorescent images were taken on a FV1000 confocal laser scanning microscope (Olympus Co., Ltd. Japan) with an objective lens. Deionized water was obtained

from Milli-Q water purification system (Millipore). pH values were measured with a Beckman Φ 50 pH meter (Shanghai LeiCi Device Works, Shanghai, China). The solutions of metal ions were prepared by using the corresponding nitrate salts.

Synthesis procedures and characterizations

Compound (1) and (2) were synthesized according to the method described in a previous literature.[30]

A solution of compound 2 (0.280 g, 1.0 mmol), 2,4-dihydroxy-1-benzaldehyde (0.249 g, 1.5 mmol) and p-methyl benzene-sulfonic acid (0.175 g, 1.0 mmol) in anhydrous ethanol (10.0 mL) were refluxed for 3 h, then the mixture was cooled to room temperature. The precipitate was filtered off, washed with anhydrous ethanol and dried in vacuum to give **Hcy-mP** as a red solid mixture (0.338 g, 85%). Mp = 226–227 °C. The structure of **Hcy-mP** was confirmed by ^{1}H NMR, ^{13}C NMR and HRMS (Fig. S7–S9†): ^{1}H NMR (600 MHz, DMSO-d_6): δ 1.60 (s, 6H, CH$_3$), 6.43–6.45 (d, J = 8.3 Hz, 1H, Ar–H), 7.10–7.12 (d, J = 15.5 Hz, 1H, CH=CH), 7.26–7.29 (d, J = 8.3 Hz, 1H, Ar–H), 7.44–7.54 (d, J = 8.1 Hz, 1H, Ar–H), 7.72–7.73 (dd, J = 8.1 Hz, 1H, Ar–H), 7.86–7.88 (d, J = 9.1 Hz, 1H, Ar–H), 7.90 (s, 1H, Ar–H), 8.52–8.54 (d, J = 16.0 Hz, 1H, CH), 10.78 (s, 1H, OH), 11.07 (s, 1H, OH). ^{13}C NMR (600 MHz, DMSO): δ 165.78, 162.49, 148.32, 147.98, 146.18, 142.14, 140.97, 138.09, 133.10, 128.53, 126.95, 125.97, 120.97, 114.52, 110.26, 107.29, 102.88, 52.27, 24.26, 21.25. HRMS (ESI-TOF) m/z calcd for $C_{18}H_{16}NO_5S^-$: 358.08; found ([M − H]$^-$): 358.0753.

General procedures for spectral determination

All spectroscopic experiments were carried out at room temperature in this paper.

4-Hydroxyethylpiperazine ethyl sulfonic acid (HEPES) was acted as buffer solution. Different concentrations (1.00 mol L^{-1}, 0.10 mol L^{-1}, 0.01 mol L^{-1}) of hydrochloric acid and sodium hydroxide were used to adjust the pH value of solution. The probe **Hcy-mP** (0.01 g) was dissolved in HEPES buffer solution (pH = 7.0) to get the stock solution (1 mM). Diluting the stock solution to make working solution (10 μM).

Calculation of association constants

Association constant (K_a) was calculated using the following equation.[31]

$$1/(F − F_0) = 1/\{K_a(F_{max} − F_0)C\} + 1/(F_{max} − F_0) \quad (1)$$

F_0 and F denote the maximum emission intensity of **Hcy-mP** (λ_{em} = 378 nm) and the observed emission intensity at the particular wavelength in the presence of certain concentration of **Hcy-mP**, respectively; F_{max} is the maximum emission intensity value that was obtained during titration with verifying analyte concentration; K_a is associate constant and was determined from the slope of the linear plot.

Calculation of detection limit

The detection limit was calculated from the fluorescence titration data based on the equation $3\sigma/K$.[32] The σ is the standard deviation of blank experiment and K is slope of the calibration curve.

Calculation of fluorescence quantum yield

The fluorescence quantum yield of **Hcy-mP** was determined according to the following equation.

$$\Phi_x = \Phi_s \frac{F_x A_s}{F_s A_x} \frac{n_x^2}{n_s^2} \quad (2)$$

where Φ is the quantum yield, F is the area under the emission spectra, A is the absorbance at the excitation wavelength, n is the refractive index of the solvent used, x subscript denotes unknown, and s means standard. The rhodamine B solution was chosen as the standard substance, Φ_s = 0.89.

Application in water samples

The tap water were obtained from school. The drinking water were obtained from our laboratory. The lake water were collected from the Labor Lake in Qiqihar. Those water samples were used without purification after static placement for 12 h. Initially, **Hcy-mP** (10 μM) was added to all the water samples (5.0 mL) followed by the addition of different concentrations (1, 3, 5 μM) of Hg^{2+}, respectively.

Cytocompatibility assay

Cell viability was used as an indicator to evaluate the cytotoxicity of fluorescent dyes for cells. In reference to these pieces of literature,[33–35] the MTT (3-(4,5-dimethylthiazol-2-yl)-2,5-diphenyltetrazolium bromide) text was used to assess the cytotoxicity of **Hcy-mP** to HeLa cells. The HeLa cells were cultured in a 96-well microplate with a density of 1.00×10^5 cells per mL at 37 °C, 5% CO$_2$. After 24 h, gently remove the medium and replace with different concentrations of **Hcy-mP** (10–100 μM) diluted in fresh medium, incubated at 37 °C for 4 h. Cells in a culture medium without **Hcy-mP** were used as the control. After washing the cells with PBS (pH = 7.4) for three times, 10 μL of MTT solution (10 mg mL^{-1}, PBS) was added into each well of the 96-well microplate, incubate for another 4 h. Then, the remaining MTT solution was removed. After shaking the plates for 10 min, the absorbance of each well was recorded with a microplate reader at 393 nm. The cell viability rate (VR) was assessed by using the following equation:

$$\% \text{ viability} = [\sum(A_i/A_{control} \times 100)]/n \quad (3)$$

where A_i is the absorbance of different concentrations of the probe of 10 μM, 20 μM, 30 μM, 40 μM and 50 μM, 60 μM, 70 μM, 80 μM, 90 μM, 100 μM, respectively. $A_{control}$ is the average absorbance of the control well in which the probe was absent, and n is the number of data point.

Intracellular culture and imaging

HeLa cells were cultured in DMEM supplement with 10% fetal bovine serum (FBS), and cells were seeded in Petri dishes and incubated at 37 °C, 5% CO$_2$ for 48 h.[36–38] Then removed culture medium, and cells were washed with PBS (pH = 7.4) for three

times.[39–43] **Hcy-mP** (10 μM) was respectively dissolved in three different pH values in PBS buffers (pH = 7.4, 3.0, 11.0) and incubated with HeLa cells for 30 min at 37 °C. Then, cells were incubated with HgCl$_2$ (10 μM) and finally incubated with EDTA (10 μM) for another 30 min. All cells were washed for 3 times with PBS before observation under microscope.[44] Fluorescence images were acquired on a confocal laser scanning microscope.

Conclusion

In summary, we designed and synthesized a highly selective and colorimetric, low cytotoxicity and water solubility probe (**Hcy-mP**) with a large Stokes shift (139 nm) using for detecting Hg^{2+} under 100% aqueous medium. The probe was used to detect Hg^{2+} *via* a turn off fluorescence, after addition of EDTA, the fluorescence recovered obviously. The detection limit of **Hcy-mP** with Hg^{2+} was reached as low as 1.08 μM. Moreover, **Hcy-mP** can be used to detect Hg^{2+} with satisfactory results in water samples. Application of **Hcy-mP** in living HeLa cells was successfully, indicating the probe has good cell membrane permeability and could be used to monitor intracellular pH fluctuations and detect Hg^{2+} in living cells.

Conflicts of interest

There are no conflicts to declare.

Acknowledgements

References

1 S. Koenig, M. Sole, C. Fernandez-Gomez and S. Diez, *Sci. Total Environ.*, 2013, **442**, 329–336.

2 L. X. Yan, Z. P. Chen, Z. Y. Zhang, C. L. Qu, L. X. Chen and D. Z. Shen, *Analyst*, 2013, **26**, 4656–4660.

3 A. Renzoni, F. Zino and E. Franchi, *Environ. Res.*, 1998, **77**, 68–72.

4 C. Y. Li, F. Xu, Y. F. Li, K. Zhou and Y. Zhou, *Anal. Chim. Acta*, 2012, **717**, 122–126.

5 J. Isaad and A. E. Achari, *Analyst*, 2013, **13**, 83809–83819.

6 T. Takeuchi, N. Morikawa, H. Matsumoto and Y. Shiraishi, *Acta Neuropathol.*, 1962, **2**, 40–57.

7 H. Matsumoto, G. Koya and T. Takeuchi, *Exp. Neurol.*, 1965, **24**, 563–574.

8 P. W. Davidson, G. J. Myers, C. Cox, C. F. Shamlaye, D. O. Marsh, M. A. Tanner, M. Berlin, J. Sloane-Reeves, E. Cernichiari, O. Choisy, A. Choi and T. W. Clarkson, *NeuroToxicology*, 1995, **16**, 677–688.

9 M. Razmiafshari, J. Kao, A. d'Avignon and N. H. Zawia, *Toxicol. Appl. Pharmacol.*, 2001, **172**, 1–10.

10 D. W. Boening, *Chemosphere*, 2000, **40**, 1335–1351.

11 H. N. Kim, W. X. Ren, J. S. Kim and J. Yoon, *Chem. Soc. Rev.*, 2012, **41**, 3210–3244.

12 M. Formica, V. Fusi, L. Giorgi and M. Micheloni, *Coord. Chem. Rev.*, 2012, **256**, 170–192.

13 Q. Lin, T. T. Lu, X. Zhu, T. B. Wei, H. Li and Y. M. Zhang, *Chem. Sci.*, 2016, **7**, 5341–5346.

14 D. Li, C. Y. Li, Y. F. Li, Z. Li and F. Xu, *Anal. Chim. Acta*, 2016, **934**, 218–225.

15 Q. Lin, X. L. Lin, T. B. Wei and Y. M. Zhang, *Chem.–Asian J.*, 2013, **8**, 3015–3021.

16 Q. X. Duan, X. Y. Lv, C. Y. Liu, Z. F. Geng, F. F. Zhang, W. L. Sheng, Z. K. Wang, P. Jia, Z. L. Li, H. C. Zhu and B. C. Zhu, *Ind. Eng. Chem. Res.*, 2019, **58**, 11–17.

17 Q. X. Duan, H. C. Zhu, C. Y. Liu, R. F. Yuan, Z. T. Fang, Z. K. Wang, P. Jia, Z. L. Li, W. L. Sheng and B. C. Zhu, *Analyst*, 2019, **144**, 1426–1432.

18 V. K. Gupta, A. K. Jain, G. Maheshwari and Z. H. Lang, *Sens. Actuators, B*, 2006, **117**, 99–106.

19 R. Joseph, B. Ramanujam, A. Acharya and C. P. Rao, *Tetrahedron Lett.*, 2009, **50**, 2735–2739.

20 M. H. Yang, P. Thirupathi and K. H. Lee, *Org. Lett.*, 2011, **13**, 5028e31.

21 J. S. Wu, I. C. H Wang, K. S. Kim and J. S. Kim, *Org. Lett.*, 2007, **9**, 907–910.

22 J. Wang, X. Qian and J. Cui, *J. Org. Chem.*, 2006, **71**, 4308–4311.

23 Y. Zhao, X. Lv, Y. Liu, J. Liu, Y. Zhang and H. Shi, *J. Mater. Chem.*, 2012, **22**, 11475e8.

24 E. M. Nolan and S. J. Lippard, *J. Am. Chem. Soc.*, 2007, **129**, 5910–5918.

25 R. Guo, J. l. Yin, Y. Y. Ma, G. H Li, Q. Wang and W. Y. Lin, *Sens. Actuators, B*, 2018, **271**, 321–328.

26 F. L. Song, X. J. Peng, E. H. Lu, R. Zhang, X. Y. Chen and B. Song, *J. Photochem. Photobiol., A*, 2014, **168**, 53–57.

27 L. Ma, Y. Li, L. Li, J. Sun, C. Tian and Y. Wu, *Chem. Commun.*, 2008, **77**, 6345–6347.

28 B. Rathinam, C. C. Chien, B. C. Chen and J. H. Liu, *Tetrahedron*, 2013, **69**, 235–241.

29 M. H. Yang, P. Thirupathi and K. H. Lee, *Org. Lett.*, 2011, **13**, 5028–5031.

30 B. Song, Q. Zhang and X. J. Peng, *J. Chem.*, 2008, **5**, 932–935.

31 Y. Kubo, M. Kato, . Misawa and W. Tokita, *Tetrahedron Lett.*, 2004, **45**, 3769–3773.

32 H. Yang, Z. Zhou, K. Huang, M. Yu, F. Li and T. Yi, *Org. Lett.*, 2007, **9**, 4729–4732.

33 W. F. Niu, Z. W. Wei, J. Jia, S. M. Shuang, C. Dong and K. M. Yun, *Dyes Pigm.*, 2018, **152**, 155–160.

34 T. Gong, R. Li, Y. Y. Yuan, B. F. Yu, H. Zhao, Z. Z Liu, R. Guo, D. Su, W. T. Liang and C. Dong, *New J. Chem.*, 2018, **42**, 12954–12959.

35 R. Guo, J. Yin, Y. Ma, Q. A. Wang and W. Lin, *J. Mater. Chem. B*, 2018, **6**, 2894–2900.

36 W. Feng, M. Li, Y. Sun and G. Feng, *Anal. Chem.*, 2017, **89**, 6106–6112.

37 Q. Xia, S. Feng, D. Liu and G. Feng, *Sens. Actuators, B*, 2018, **258**, 8–104.

38 B. Huang, W. Chen and Y. Q. Kuang, *Org. Biomol. Chem.*, 2017, **15**, 4383–4389.

39 D. Xu, Y. H. Li, C. Y. Poon, H. N Chan, H. W. Li and M. S. Wong, *Anal. Chem.*, 2018, **90**, 8800–8806.

40 S. V. Mulay, M. Choi, Y. J. Jang, Y. Kim, S. Jon and D. G. Churchill, *Chem.–Eur. J.*, 2016, **22**, 9642–9964.

41 J. B. Chao, K. L. Song, Y. B. Zhang, C. X. Yin, F. J. Huo, J. J. Wang and T. Zhang, *Talanta*, 2018, **189**, 150–156.

42 W. Niu, L. Fan, M. Nan, M. S. Won, S. Shuang and C. Dong, *Sens. Actuators, B*, 2016, **234**, 534–540.

43 F. Meng, Y. Liu, J. Niu and W. Lin, *Tetrahedron Lett.*, 2017, **58**, 3287–3293.

44 Z. X. Tong, W. Liu, H. Huang, H.-Z. Chen, X.-J. Liu, Y.-Q. Kuang and J.-H. Jiang, *Analyst*, 2017, **142**, 3906–3912.